Geotechnical Aspects of Underground Construction in Soft Ground, Kusakabe, Fujita & Miyazaki (eds)
© 2000 Balkema, Rotterdam, ISBN 90 5809 1 066

Earth pressures acting on a deep shaft and the movements of adjacent ground in sand

S. Imamura, T. Nomoto, T. Fujii & T. Hagiwara
Nishimatsu Construction Company Limited, Tokyo, Japan

O. Kusakabe
Department of Civil Engineering, Tokyo Institute of Technology, Japan

ABSTRACT: A series of centrifuge model tests was carried out in an attempt to evaluate earth pressures acting on a deep circular shaft in dry sand up to prototype depth of 50 m and associated ground deformation. Based on the test results combined with the data obtained from the previous centrifuge tests by the authors, the active earth pressures and failure mechanism for a deep circular shaft in sandy ground are proposed.

1 INTRODUCTION

In recent years, large-scale shaft construction projects, of which excavation depth is 50 m or more, have been extensively carried out because of rapid increase in underground space development. However, in the case of such construction projects, current environment requirements impose strict restrictions on ground deformation and movement of existing structures. Therefore, to meet these criteria, it is extremely important to accurately evaluate ground movements around the shaft, together with earth pressures acting on the shaft lining.

A number of studies has been conducted to understand the behaviour due to excavation work. However, there are still a limited number of field data with the detailed monitoring during the construction work to date. In addition, the precise design method based on the quantitative evaluation of earth pressures acting on a very deep shafts and the surrounding ground deformation has yet to be established.

The authors have been accumulating a large amount of experimental data related to active earth pressures on an axisymmetric deep shaft in dry sand and associated ground deformation by a series of centrifuge studies since 1990. Up to now, active earth pressures on the axisymmetric shaft up to the prototype depth of 30 m were successfully measured (Fujii et al.,1994, Fujii et al., 1996, Hagiwara et al., 1998). The accuracy of the test results was stepwise improved and their adequacy was also confirmed by comparing with FEM analysis, using a three dimensional elasto-plastic model (Hagiwara et al.,1994). The authors have become strongly aware that detailed observations in physical modelling are absolutely important to evaluate earth pressures and surrounding ground deformations due to deep shaft construction, and beneficial for actual designers who tackling large scale excavation projects.

This paper briefly describes the updated centrifugal testing system to model the shaft of 50 m in prototype depth and discusses the test results, putting an emphasis on earth pressures acting on the shaft lining and associated ground deformations.

2 CENTRIFUGE MODEL TESTS

2.1 *Model shaft and Equipments*

Figure 1 shows a general arrangement for centrifuge model tests. The centrifuge model tests were carried out at Nishimatsu dynamic geotechnical centrifuge (Imamura et al., 1998). Its effective radius is 3.80 m and the maximum pay load capacity 19.2 MN-m/sec^2. The model shaft, made of duralumin, consists of two semi-cylinders to allow one of the semi-cylinders to move horizontally. The shaft of 120 mm diameter and 500 mm height had enough rigidity. The maximum initial distance between the stationary part and the moving part was 40 mm so that could investigate the failure mechanism of model ground around the shaft. Ten small size stress transducers (24 mm width $\times$ 10 mm height) capable of measuring horizontal earth pressure were embedded in the moving part of the shaft at 50mm intervals. The maximum capacity of the transducers was 392kN/m^2.

2.2 *Test procedures*

Centrifuge test procedures were generally as follows: The soil used in the experiments was air-dried Toyoura sands. The material properties of Toyoura sands are shown in Table 1. The model ground was prepared

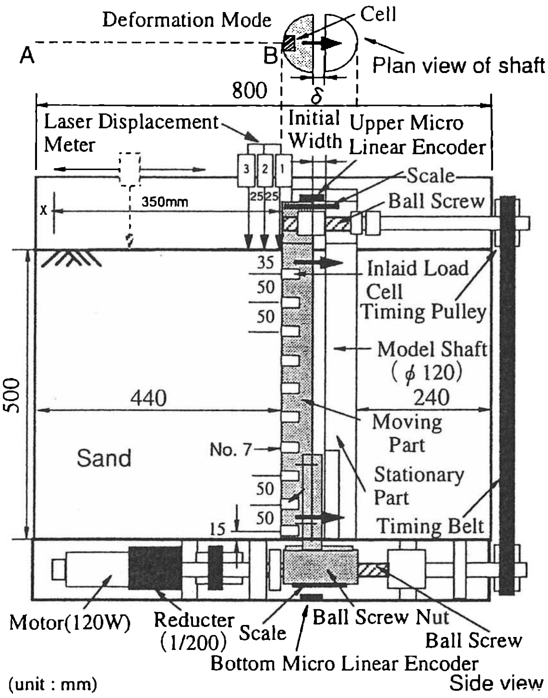

Figure 1. Schematic of centrifuge model and instrumentation.

by pouring these sands to achieve their unit weight γ_d of 15.2 kN/m^3 (Dr = 70 %) in each test. In one of tests, colored-sand layers of 2 mm thick and small lead shots(Diameter = 2 mm) were horizontally placed in the ground at intervals of 25 mm in order to investigate the ground movements around the shaft. The centrifuge was accelerated to 981m/s^2 (100 g) in about 15 minutes. An uniform movement of the moving part was achieved from top to bottom of the shaft, using the ball screw with a constant rate of 0.75 mm/min. Earth pressures at rest, and during lateral shaft movement of up to 3.6 mm were carefully measured at ten locations on the shaft lining. Three laser displacement meters with a resolution of 0.01 mm were employed in order to measure the ground surface movements around the shaft. After the experiment, the model sand was turned round, and carefully vacuumed with an air cleaner along the central vertical plane to make it possible to closely observe the extent of the failure zones after for active deformation.

The centrifuge test conditions as well as the examination points are summarized in Table 2. Four tests were performed to investigate active earth pressures acting on the shaft lining (50 m in prototype depth), earth pressures in the model ground and ground movements around the shaft. Check of Modelling of models on this centrifuge model had been conducted and the validity of its scaling relations for both active earth pressure distributions and failure mechanisms been confirmed (Hagiwara et al.,1998).

Table 1. The material properties of Toyoura sands.

Specific density, ρ_s	2.63
Maximum void ratio, e_{max}	0.961
Minimum void ratio, e_{min}	0.593
Coefficient of uniformity, Uc	1.41
D_{50}, (mm)	0.18
Internal friction angle, ϕ'_{max}(°), (Dr=70%)	42

Table 2. The centrifuge test conditions.

Code	Acceleration a (m/s^2)	Prototype shaft Diameter(m), Depth(m) (Model size)	Unit weight γ_d (kN/m^3)	Maximum displacement δ (10^{-3} m) (Model, mm)	Main theme
SA−1 SA−2 SA−3	981 (100g)	Dp=12 (D=120mm) Zp=50 (H=500mm)	15.2 15.2 15.2	360 (3.6)	Earth pressure Ground deformation
SA−4	981 (100g)	Dp=12 Zp=50	15.3	1000 (10)	Earth pressure Failure mode

3 TEST RESULTS AND DISCUSSIONS

3.1 *Failure mechanisms*

Figure 2 shows failure mechanism at the central vertical plane around the shaft(A-B section in Figure 1). In addition, Figure 3 shows observed sub-surface deformation obtained from lead shot's movements, together with the failure mechanism proposed by the previous study(Fujii et al., 1996). The failure surface at upper portion develops approximately along the shaft lining as rigid block, having constant width regardless of the shaft depth. At greater depths, the dominant rupture surface seems to be approximated as a logarithmic spiral curve, as shown in Figure 3. It is clear from Figure 3 (left side) that the failure region extends to the distance of about 0.30D (D: shaft diameter) from the shaft lining. This region is much smaller than that of two-dimensional failure mechanism based on the centrifuge model tests of slurry trenches by Tohda et al.(1991). This failure pattern is consistent with the previous results based on the models having the different prototype depths (10 m, 20 m, 30 m). Therefore, it can be inferred that the failure mechanism, as shown in Figure 3, is unique one regardless of the shaft depth.

Figure 3(right side) shows the distribution of maximum shear strain rates γ (relative values) by the finite element method (Hagiwara et al.,1998). This result was based on a three-dimensional elasto-plastic model. The observed failure mode compares favorably with that obtained from FEM.

3.2 *Influence zone of failure*

Figure 4 illustrates the relationship between the distance from the shaft normalized by diameter D and

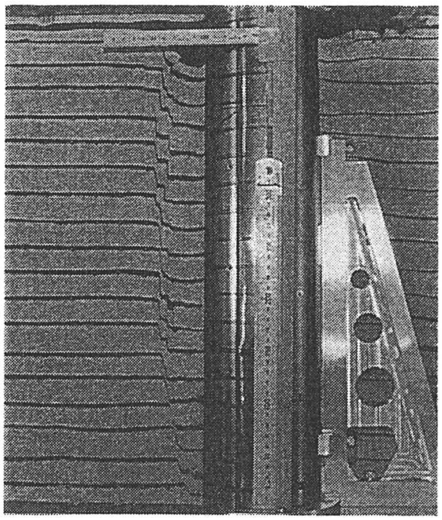

Figure 2. Failure pattern (Diameter 12m, Depth 50 m).

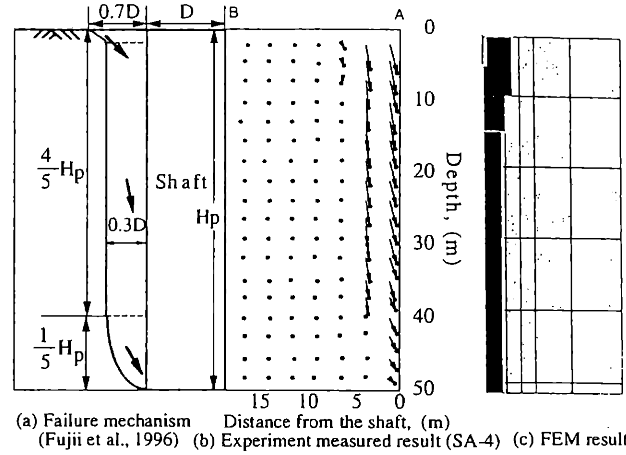

Figure 3. The failure mechanism and sub-surface deformation at the active state.

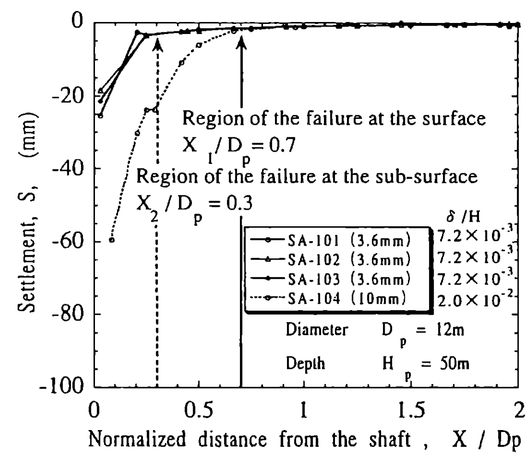

Figure 4. Ground surface settlement profiles.

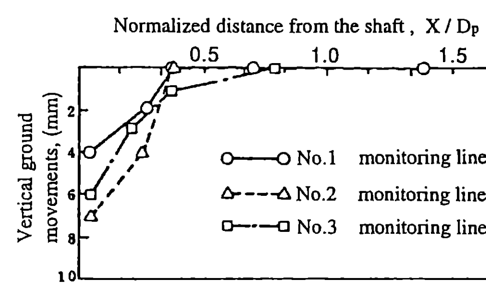

Figure 5. Ground surface settlement profiles (field data, Matsuoka et al., 1996).

ground surface settlements around the shaft. From the figure(SA-1 ~ 4), the surface settlements in every case increase rapidly at $X_2 / D_p \fallingdotseq 0.3$. On the other hand, in the case of SA-4, the surface settlement sharply increases at both $X_2 / D_p \fallingdotseq 0.3$ and $X_1 / D_p \fallingdotseq 0.7$, and clear failure zone at the surface, having large settlements is observed. These kinky points correspond well with failure region at the surface and sub-surface(see Figure 3). Hence, the surface settlement increases rapidly at $X / D_p \fallingdotseq 0.3$ regardless of strain level of the shaft movement for all the tests. Therefore, this distance can be regarded as an index of failure sphere in the ground around the shaft.

Figure 5 shows the ground surface settlement profiles at the central section after the construction with the field data obtained from the large-scale shaft construction (Diameter=30.6m, GL-60.3 m in excavation depth) in an alluvial sandy soil (Matsuoka et al., 1996). Apart from the amount of settlement, the field data and the centrifuge results (Figure 4) show a similar trend, especially on the kinkiy points at $X_2 / D_p \fallingdotseq 0.30$ (failure zone).

Figure 6 shows the relationship between the changeover depth and the distance from the shaft X_1 at the surface normalized by depth H_p, and the normalized distance X_2 / H_p at the sub-surface ground, together with the previous centrifuge results(shaft depth of H_p = 10, 20, 30 m). In addition, zones of recent neighboring construction guide and of a two-dimensional active failure line ($\pi / 4 + \phi ' / 2$) are shown for comparison. In all the cases, the horizontal earth pressures acting on the shaft lining reached to active state at strain level of around $\delta / H = 2.0 \times 10^{-3}$ (δ : horizontal displacement, H: height of the shaft). At this point, in due consideration of actual strain level of the shaft, X_2 is taken up as the region of influence. It can be seen from Figure 6 that X_2 / H_p values are almost constant regardless of the shaft depth, having an average value of 0.10. As compared with the recommended value at the recent neighboring construction principle, the experimental value is much smaller, showing about 30 percent order of the recommended one. It is indicated that the current design method overvalues the failure zone around the deep circular shaft.

Figure 7 also shows the relationship between the changeover depth and the distance from the shaft X_1 at the surface normalized by diameter D_p, and the normalized distance X_2 / D_p at the sub-surface, together with numerical results based on the finite element analysis(Hagiwara et al.,1998) and the field data (Matsuoka et al., 1996). The overall values of X_2 / D_p

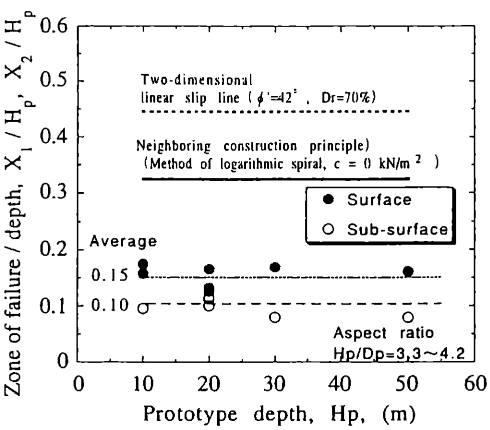

Figure 6. Relationship between the changeover depth and zone of failure normalized by H_p.

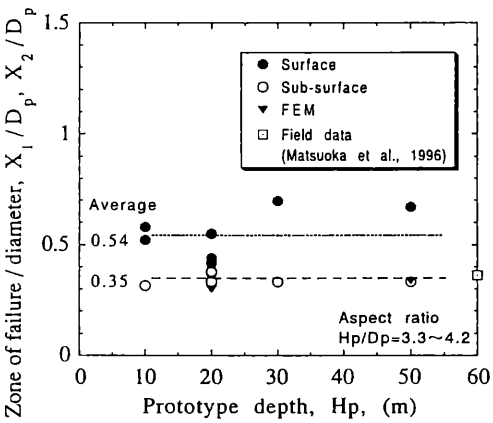

Figure 7. Relationship between the changeover depth and zone of failure normalized by D_p.

show a similar tend, giving a constant value of 0.35 (the average value). Accordingly, it is suggested that influence zone of failure with the shaft construction up to 50 m in depth is approximately $0.35D_p$ regardless of stress level and peripheral ground deformations are more dominated by the three-dimensional shape effect of shafts. Furthermore, the measured influence zone of failure at the sub-surface is in good agreement both numerical result and field data.

3.3 *Distributions of active earth pressure*

Figure 8 shows the change of earth pressure distributions from the initial state at rest to the active state for the prototype depth of 50 m. Horizontal earth pressures σ_h on the shaft lining are plotted versus prototype normalized depth Z/H_p, together with Rankine's active earth pressure, the earth pressures calculated from Beresantsev's solution (1958) for the circular shaft and numerical results based on finite element analysis (Hagiwara et al., 1998).

Earth pressures at rest increase linearly with depth and generally agree with the earth pressure distributions based on Ko (=0.33) given by Jaky's

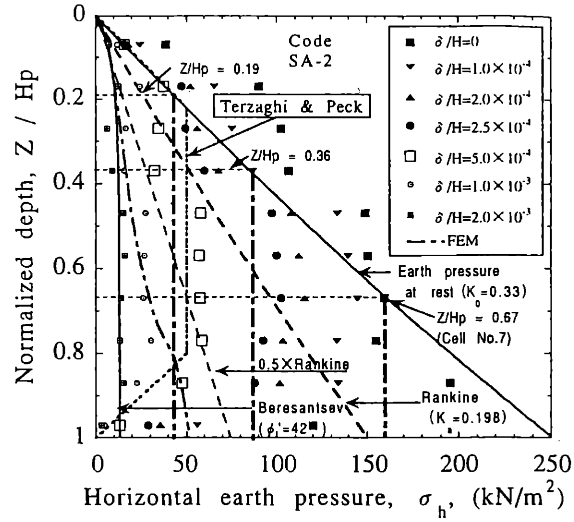

Figure 8. Active earth pressure distributions (50 m).

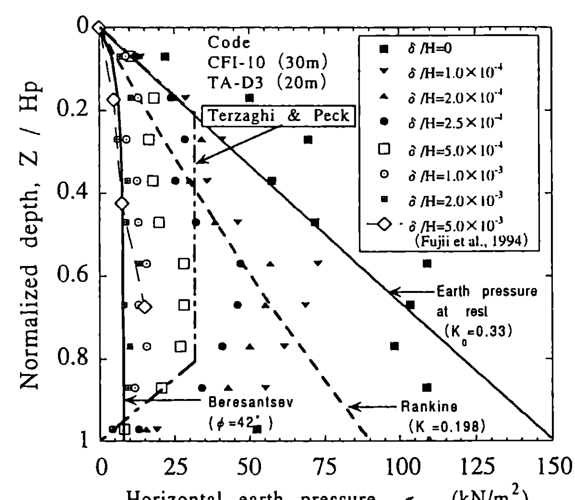

Figure 9. Active earth pressure distributions (30 m).

equation (Ko =1-sin ϕ', $\phi' = 42°$). Earth pressure distributions gradually approach Beresantsev's results, as the horizontal displacement of the shaft (δ) increases. Furthermore, Terzaghi & Peck's prediction, earth pressure distribution(1967) based on axial force of field data, is also presented in this figure. The overall shape of earth pressure distributions at strain level of δ / H=5.0 $\times 10^{-4}$ has corresponds to well to that based on Terzaghi & Peck's method. The measured earth pressure distributions at strain level of δ / H=2.0 $\times 10^{-3}$ coincide well with the results based on Beresantsev's formula and FEM. Experimental results are much smaller than Rankine's two-dimensional result. The reason may be the redistribution of stress at the deeper points is made by means of arching effects which developed with the movement of the shaft lining.

This tendency of earth pressure distribution having constant value is similar to the field data down to about GL-10 m in sandy soil (Enami at al., 1996) obtained from the caisson construction (Diameter 30.4 m, GL-36.2 in excavation depth) .

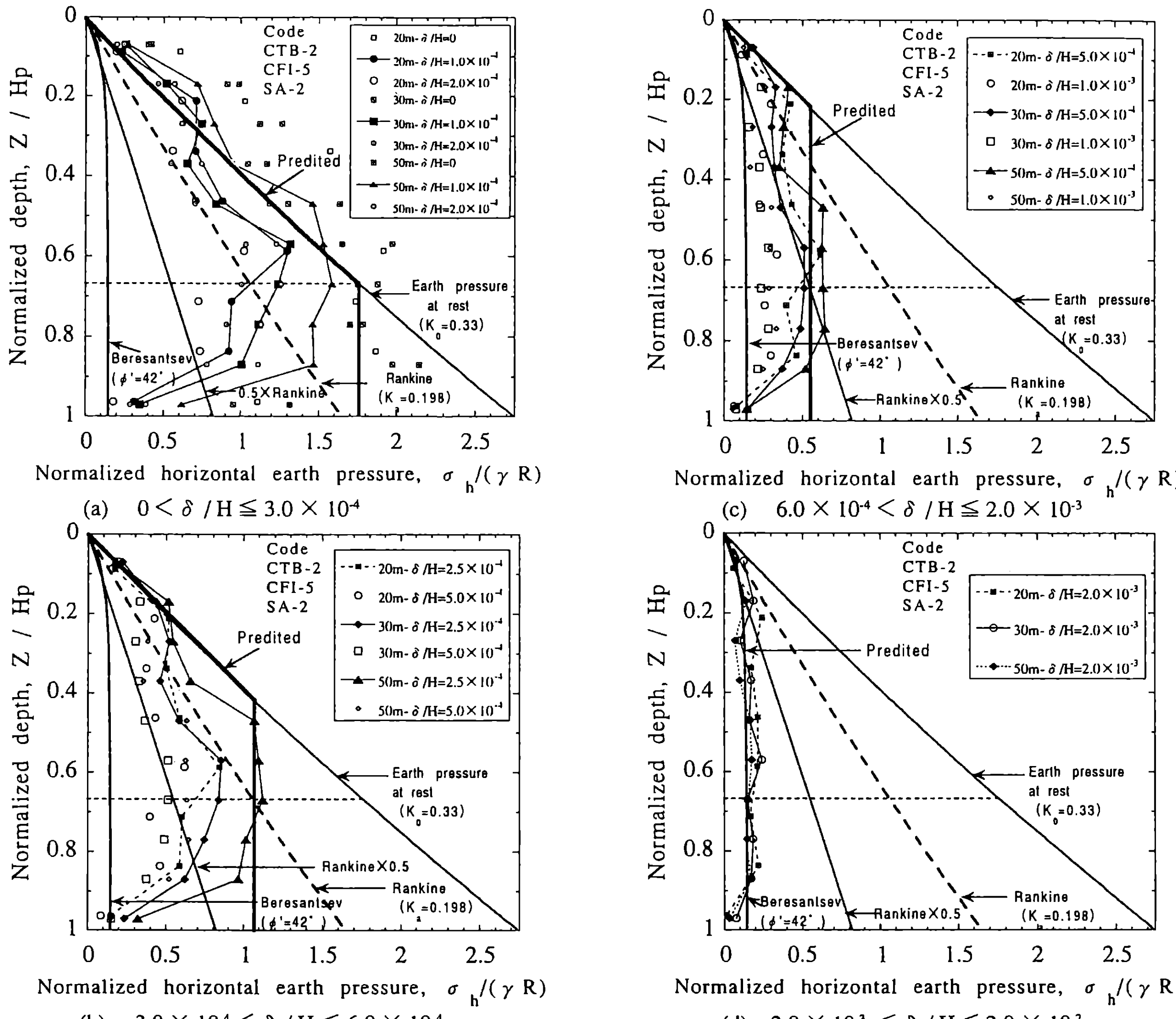

Figure 10. Predicted and active earth pressure distributions according to strain level.

It is clearly found that the active earth pressure given by Rankine's two dimensional theory tends to overestimate the active earth pressures on a deep circular shaft, especially at deeper depth. Therefore, three-dimensional effects must be fully taken into account in the case of deep circular shafts for prototype depths up to 50 m. These observed active earth pressure distributions agree fairly with the centrifuge data given by Lade et al.(1981) and Fujii et al.(1994).

In the same manner as Figure 8, Figure 9 shows the results of active earth pressures from the previous centrifuge studies. The results of the active earth pressure distribution and the process from the initial state at rest to active state for the prototype depth of 50 m agree well with the previous data(CFI-10, TA-D3). It is confirmed that the active earth pressure is constant and coincides well with the results based on Beresantsev's formula independent of the depth up to 50m. Therefore, it was revealed that these centrifuge tests provided reliable data in horizontal earth pressures for deep circular shafts in dry sand, as well as the validity of the testing system.

3.4 *An experimental prediction method of earth pressures acting on the shaft*

An experimental prediction method for earth pressure acting on the shaft was made based on this study. The concept of this method is mentioned as below.

The values of earth pressure tend to in the initial state at rest become greater independent of test cases(see Figures 8 – 9). This trend is clearly observed over the shallower half. Because the model sand is made in the state of over consolidation in gravity, the model ground is not normally consolidated over the shallower half regardless of a high centrifugal field. In contrast, earth pressure at the lowest point is very small in all cases because of boundary condition in model. Consequently, it is assumed that soil condition is judged by cell No.7 at the most stabilized point of all the earth pressures.

From three test cases(SA-1 ~ 3), the horizontal earth pressure immediately after deformation of the shaft, and the earth pressure at strain level of $\delta/H = 3.0 \times 10^{-4}$, 6.0×10^{-4}, which earth pressure at the point of No.7 is equal to be Rankine' s earth pressure, a half Rankine' s earth pressure, are denoted as dashed and single-dotted line in Figure 8. The depth crossing Jaky' s Ko-line at each stress level can be demonstrated in Figure 8. Hence, the authors assumed Jaky's equation up to depth at cross point, and constant value down to cross point according to strain level in the light of failure process around the shaft.

Finally, we obtained an expression for the values of the normalized horizontal earth pressure $\sigma_h / \gamma R$ according to strain level of δ/H in dependent of depth, that is, stress level.

(1) $0 < \delta / H \leqq 3.0 \times 10^{-4}$
i) $0 \leqq Z/Hp \leqq 0.67$ $(=\alpha)$、ii) $0.67 \leqq Z/Hp \leqq 1.0$
(2) $3.0 \times 10^{-4} < \delta / H \leqq 6.0 \times 10^{-4}$
i) $0 \leqq Z/Hp \leqq 0.36$ $(=\beta)$、ii) $0.36 \leqq Z/Hp \leqq 1.0$
(3) $6.0 \times 10^{-4} < \delta / H \leqq 2.0 \times 10^{-3}$
i) $0 \leqq Z/Hp \leqq 0.19$ $(=\lambda)$、ii) $0.19 \leqq Z/Hp \leqq 1.0$
(4) $2.0 \times 10^{-3} \leqq \delta / H \leqq 2.0 \times 10^{-2}$, $0 \leqq Z/Hp \leqq 1.0$
(1)~(3)
i) $\sigma_h / (\gamma R) = Ko\ (Hp/R) \times (Z/Hp)$
ii) $\sigma_h / (\gamma R) = (\alpha, \beta, \lambda) \times Ko\ (Hp/R)$
(4) $\sigma_h / (\gamma R) = \sigma_B / (\gamma R)$

where σ_B is Beresantsev's solution in the state of active earth pressure, R : the radius of the shaft, γ : the unit weight of the soil, α, β, λ : coefficient

Figures 10 (a) — (d) are plotted the test results of 20 m(CTB-2), 30 m(CFI-5), and 50 m(SA-2) in depth with the displacement of the shaft (δ /H) , together with predicted distribution as thick solid line. It can be concluded that the predictive method proposed by the centrifuge study gives a rational estimation of horizontal earth pressures acting on the shaft as the need strain level of δ / H regardless of the shaft depth. It is known that the stain level δ / H of the actual shaft is about $1.0 \times 10^{-4} \sim 5.0 \times 10^{-4}$ (maximum of horizontal displacement : 5 ~ 25mm, Enami et al.,1996) regardless of excavation depth. Design chart equivalent to this strain level is shown in Figures 10 (a) and (b) . This proposed method provides a conservative prediction of the horizontal earth pressure acting on an axisymmetric deep shaft.

4 CONCLUSIONS

The knowledge gained by this study is outlined as follows.

1. The active failure mechanism of the sub-ground around the circular shaft, having the prototype depth of 50 m, was well consistent with that obtained from the previous centrifuge studies aimed at the shafts below 30 m in depth. Moreover, validity and reliability of the centrifuge model tests was confirmed.

2. Zone influence of active failure due to the shaft construction in sandy ground is approximated as 0.35D independent of stress level up to the shaft depth of 50m.

3. Measured values of horizontal earth pressure acting on a circular shaft coincided well with axisymmetric calculations based on Beresantsev's formula and the numerical values from an elasto-plastic FE analysis. Current design codes, based on conventional two-dimensional models, overestimated the active earth pressure acting on a circular shaft, especially at deeper positions.

4. The experimental prediction charts to estimate the active earth pressure distributions acting on the deeper shaft were drawn by taking into consideration of strain level of the shafts. This proposed method provides a rational and conservative prediction of the horizontal earth pressure acting on an axisymmetric deep shaft according to strain level of the shaft.

ACKNOWLEDGEMENTS

The authors wish to thank Professor N. Fujii of Chuo University, Professor K. Ugai of Gunma University and Lecturer K. Ueno of Tokushima University for their encouragement and helpful suggestions in the preparation of this paper.

REFERENCES

Berezantsev, V.G. 1958. Earth pressure on the cylindrical retaining walls, *Brussels Conf. on Earth Pressure Problems*, :21- 27.

Enami, A., H. Morishita, M. Ogihara, M. Homma, H. Tezuka, Y. Hiramatsu 1996. Earth pressure acting on a deep circular shaft wall, *Proc. of Geotechnical Aspects of Underground Construction in Soft Ground* :117-122.

Fujii, T., T. Hagiwara, K. Ueno & A. Taguchi 1994. Experiment and analysis of earth pressure on axisymmetric shaft in sand, *Proc. of Centrifuge 94*: 791-796.

Fujii, T., T. Hagiwara & O. Kusakabe 1996. Active failure mechanism of a deep circular shaft in dry sand, *Proc.of Geotechnical Aspects of Underground Construction in Soft Ground*:137-142.

Hagiwara, T., S. Imamura, T. Fujii, T. Nomoto & O. Kusakabe 1998. Earth pressure acting on a deep circular shaft and associated ground deformation, *Proc. of Centrifuge 98*: 643-648.

Hagiwara, T., K. Ugai, T. Fujii & M. Ishibashi 1994. Numerical simulation of centrifugal model tests on earth pressure of a deep shaft in dry sand by elasto-plastic FEM, *Proc. of the 8th IACMAG*, (Ⅱ) :1731-1736.

Imamura, S., T. Hagiwara, & T. Nomoto 1998. Nishimatsu dynamic geotechnical centrifuge facility, *Proc. of Centrifuge 98*: 19-24.

Lade, P.V., H.L. Jessberger, E. Makowski & P. Jordan 1981. Modeling of deep shafts in centrifuge tests, *Proc. 10th ICSMFE*, (1) :683-691.

Muramatsu, M. & Y. Abe 1996. Considerations in shaft excavation and peripheral deformation, *Proc. of Geotechnical Aspects of Underground Construction in Soft Ground* (Mair and Taylor eds):173-178.

Terzaghi, K. & R. B. Peck 1967. *Soil Mechanics in Engineering Practice*, John Wiley & Sons.

Ueno, K., K. Yokoyama, A. Ohi & T. Fujii 1996. Earth pressures acting on flexible circular shafts in sand, *Proc. of Geotechnical Aspects of Underground Construction in Soft Ground* (Mair and Taylor eds): 237-242.